Available online at www.sciencedirect.com

ScienceDirect

Advances in Space Research 62 (2018) 1191–1202

ADVANCES IN SPACE RESEARCH (a COSPAR publication)

www.elsevier.com/locate/asr

Mapping ice sheet grounding lines with CryoSat-2

Anna E. Hogg [a,*], Andrew Shepherd [a], Lin Gilbert [b], Alan Muir [b,c], Mark R. Drinkwater [d]

[a] Centre for Polar Observation and Modelling, School of Earth and Environment, University of Leeds, Leeds LS2 9JT, UK
[b] Mullard Space Science Laboratory, University College London, Holmbury Hill Rd, Dorking, Surrey RH5 6NT, UK
[c] Centre for Polar Observation and Modelling, University College London, Gower Street, London WC1E 6BT, UK
[d] European Space Agency, ESA-ESTEC, Kelperlaan 1, 2201 AZ Noordwijk, Netherlands

Received 5 September 2016; received in revised form 6 March 2017; accepted 8 March 2017
Available online 18 March 2017

Abstract

The boundary between grounded and floating ice is an important glaciological parameter, because it delineates the lateral extent of an ice sheet and it marks the optimal location for computing ice discharge. We present a method for detecting the grounding line as the break in ice sheet surface slope, computed from CryoSat-2 elevation measurements using a plane-fitting solution. We apply this technique to map the break in surface slope in four topographically diverse sectors of Antarctica - Filchner-Ronne Ice Shelf, Ekström Ice Shelf, Amundsen Sea sector, and the Larsen-C Ice Shelf - using CryoSat-2 observations acquired between July 2010 and May 2014. An inter-comparison of the CryoSat-2 break in surface slope with independent measurements of the hinge line determined from quadruple-difference SAR interferometry (QDInSAR) shows good overall agreement between techniques, with a mean separation of 4.5 km. In the Amundsen Sea sector, where in places over 35 km of hinge line retreat has occurred since 1992, the CryoSat-2 break in surface slope coincides with the most recent hinge line position, recorded in 2011. The technique we have developed is automatic, is computationally-efficient, can be repeated given further data, and offers a complementary tool for monitoring changes in the lateral extent of grounded ice.

Keywords: Altimetry; CryoSat-2; Grounding line; Slope

1. Introduction

Grounding lines mark the boundary between floating and grounded sections of a marine terminating ice sheet (Thomas et al., 1979). They are a sensitive indicator of ice sheet stability and, when migration occurs, can indicate the influence of changes in the local environmental forcing (Joughin et al., 2010, 2012, 2014; Dutrieux et al., 2014). Monitoring changes in grounding line positions allows regions of instability to be identified, and such measurements are a valuable reference for assessing the fidelity of ice dynamical models (Favier et al., 2014). The location of the grounding line can fluctuate over short (sub-daily) timescales, due to the effects of ocean tides and localised variations in ice thickness (Hogg et al., 2016), and over longer (annual to decadal) timescales, if sustained changes in ice thickness occur (Rignot, 1998b; Park et al., 2013; Rignot et al., 2014). The grounding line lies at the landward edge of a zone where ice shelf flexure occurs as a consequence of ocean height variations, for example due to tidal displacement, the inverse barometer effect, and oceanic circulation variability. This flexure zone can be over 4 km wide in the flow-line direction (Hogg et al., 2016) depending on factors such as bed topography, ice thickness and tide amplitude (Rignot, 1998b). Although

* Corresponding author. Fax: +44 (0)113 343 5259.
E-mail addresses: A.E.Hogg@leeds.ac.uk (A.E. Hogg), A.Shepherd@leeds.ac.uk (A. Shepherd), L.Gilbert@ucl.ac.uk (L. Gilbert), a.muir@ucl.ac.uk (A. Muir), Mark.Drinkwater@esa.int (M.R. Drinkwater).

http://dx.doi.org/10.1016/j.asr.2017.03.008
0273-1177/

grounding lines cannot be directly observed because they lie at the base of the ice sheet, their surface expression - the hinge line - can be detected using a range of in situ and remote-sensing techniques (Vaughan, 1995; Rignot, 1998b; Fricker and Padman, 2006). Although there may be small departures between the lateral positions of hinge- and grounding-lines (Fig. 1), in areas of high basal shear their migration rates are similar, and so tracking hinge line movement is an accurate measure of grounding line migration or stasis (Rignot, 1998b).

Three techniques have been used to map ice sheet grounding lines using satellite observations; quadruple difference interferometric synthetic aperture radar (QDInSAR) (Rignot, 1998a, 2011), laser altimetry (Fricker and Padman, 2006; Horgan and Anandakrishnan, 2006; Fricker et al., 2009; Brunt et al., 2010, 2011) and shadows in optical satellite imagery (Scambos et al., 2007; Bohlander and Scambos, 2007); or a combination of multiple techniques (Bindschadler et al., 2011). Each approach has strengths and weaknesses. Although QDInSAR provides a precise measurement of relative tidal displacement with fine spatial resolution, the spatial and temporal extent of suitable data is relatively poor, and there are few regions where the method has been applied repeatedly. Ice shelf tidal displacement is also detectable in repeat laser altimetry (Fricker and Padman, 2006). The most extensive assessments are based on measurements acquired by the Ice, Cloud, and land Elevation Satellite (ICESat), but the mission lifetime was relatively short (~6 -years), and the ground track coverage is relatively sparse. Finally, when favourably illuminated, the break in ice sheet surface slope which often occurs in the vicinity of the grounding line causes shadows in cloud-free optical satellite imagery (Scambos et al., 2007). This feature has been used to delineate the break in slope as a proxy for the grounding line position, however; the manual technique is laborious and not easily repeatable. The Antarctic Surface Accumulation and Ice Discharge (ASAID) project has produced a continuous grounded ice boundary for Antarctica through manual delineation of the shadow edge boundary, modulated with repeat track laser altimetry data when available (Brunt et al., 2010), and this product agrees well with the QDInSAR grounding line in steeply slope regions (Bindschadler et al., 2011). While progress has been made using all three techniques, to date the spatial and temporal extent of grounding line data sets remains sparse, and a method for continuously monitoring long term change in grounding line position is still required. Consequently there is a high priority need for a robust, all-weather, year-round technique by which to autonomously and repeatedly retrieve a contiguous Antarctic grounding line.

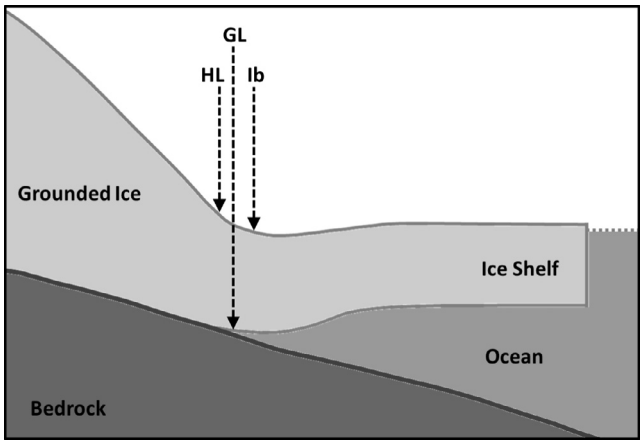

Fig. 1. Illustration showing the location of the ice sheet grounding line (GL), hinge line (HL), break in surface slope (Ib) (adapted from Bindschadler et al., 2011).

In areas of high basal shear, the ice surface evolves in response to changes in grounding line location (Schoof, 2007; Joughin et al., 2010), and this relationship is the motivation for the use of the break in surface slope (Ib) (Fig. 1) as a proxy for the grounding line position (Bindschadler et al., 2011). Here, we develop a computationally efficient, automated method for mapping the break in slope using geodetic surface height measurements to assess the validity of this assumption. We map the break in slope using CryoSat-2 data in four topographically diverse study areas of Antarctica, the Amundsen Sea sector, and the Filchner-Ronne, Larsen-C and Ekström Ice Shelves. We evaluate the extent to which the break in surface slope coincides with the hinge line located using QDInSAR (Rignot et al., 2011), and the shadow edge boundary modulated with repeat track laser altimetry (Bindschadler et al., 2011).

2. Data

We use ~3.8 years of CryoSat-2 Baseline-B intermediate Level 2 (L2i) Synthetic Aperture Radar Interferometric (SARIn) mode radar altimeter measurements of ice sheet surface elevation, acquired between 16th July 2010 and 4th May 2014, as the basis for our slope calculation. The acquisition date and time, latitude and longitude at the slope-corrected point of closest approach (POCA), surface height with respect to the ellipsoid, and the radar backscatter coefficient are obtained for each CryoSat-2 SARIn data point in all four areas of interest. Poor quality data is removed using the measurement confidence, measurement quality, retracker and corrections error flags provided in the L2i CryoSat-2 metadata, all of which are set to zero if the data quality is good. In total 3.7% of the input CryoSat-2 data was removed using the data quality flags. The range between the CryoSat-2 satellite and the ice surface is corrected for fluctuations in dry and wet tropospheric mass, the effect of the ionosphere, inverse barometric atmospheric pressure variations, and the solid Earth and ocean loading tides (Table 1). The elevation measurement is re-tided by subtracting the long period equilibrium ocean, geocentric polar and ocean tide geophysical corrections applied as default in the ESA CryoSat-2 data product. The ocean tide amplitude is then

Table 1
Geophysical corrections applied to the CryoSat-2 data and their typical range (ESA, 2012).

Correction	Minimum (cm)	Maximum (cm)
Dry troposphere	170	250
Wet troposphere	0	37
Ionosphere	6	12
Inverse barometric	−15	15
Solid Earth tide	−30	30
Geocentric polar tide	−2	2
Ocean loading tide	−2	2
Ocean tide (CATS2008a)	−50	50

simulated and removed from the CryoSat-2 surface elevation measurement using the independent CATS2008 ocean tide model, which is an updated version of the data assimilation model described by Padman et al. (2002). We use the CATS2008 ocean tide correction rather than the FES2004 ocean tide correction provided with CryoSat-2 because the spatial extent of the CATS2008 model domain matches the known ocean - land boundary in Antarctica in areas where the corresponding CryoSat-2 geophysical correction is not provided, and the phase and amplitude of the CATS2008 tide model is more accurate than other tide model simulations in coastal Antarctica (McMillan et al., 2011).

The novel SARIn mode on CryoSat-2 improves sampling density in the topographically heterogeneous ice sheet margins, making it particularly well suited for mapping slope in areas of steeply sloping terrain relative to conventional pulse limited altimeter missions (Wingham et al., 2006). The surface elevation measured by traditional pulse limited altimeters, such as ERS-1/2, is the height of the closest point within the altimeter footprint, the size of which is determined by the altimeter instrument characteristics such as operating frequency and platform imaging geometry. The CryoSat-2 SAR Interferometric Radar Altimeter (SIRAL) instrument operates in SARIn mode in the ice sheet margins, and Low Rate Mode (LRM) in the ice sheet interior. The return radar signal reflected off the ice surface is received by two SIRAL antennas mounted with a baseline separation of ~1.2 m across the flight direction of the CryoSat-2 satellite (ESA, 2012). Any difference in the return signal time is caused by differences in the path length travelled, and such differences in travel time can only result in the return signal if the echo originates from an off-nadir location. The POCA, the across track location within the 0.3 km (along track) by 1.5 km (across track) CryoSat-2 footprint, can therefore be determined from the phase and angle of arrival of the return signal (Wingham et al., 2006). Furthermore, CryoSat-2 is operated in a 369-day drifting orbit with a 30-day sub cycle. The novel POCA retrieval combined with a drifting orbital cycle dramatically improves the spatial coverage of radar altimetry measurements retrieved in the ice sheet margins, increasing from 10% by ENVISAT to 49% by CryoSat-2 (McMillan et al., 2014). In the vicinity of the grounding line CryoSat-2 SARIn mode achieves an average data density of 302 points per 25 km^2 based on the full dataset used in this study (Fig. 2).

An artefact of the SARIn acquisition mode is that high elevation topographic features, such as mountain ridges, are preferentially sampled relative to their surrounding terrain. This is particularly noticeable in the Larsen-C and Ekström Ice Shelf study areas (Fig. 2d and e) where there is a high density of POCA acquired along the spine of the Antarctic Peninsula and the Sorasen Ridge, respectively. The disadvantage of this is that the area surrounding prominent topographic features are rarely or never sampled as the POCA, leaving these regions unobserved by standard retracking of the CryoSat-2 SARIn mode data. In regions with complex mountainous terrain we also find a much higher incidence of elevation measurement retrieval error, which in Level 2 CryoSat-2 SARIn mode data is visible as a point located on the default nadir ground track. A CryoSat-2 measurement is deemed to be in error if the surface elevation differs by more than 50 m from an auxiliary 1 by 1 km grid resolution Digital Elevation Model (DEM). The Antarctic Peninsula is ~70 km wide with mountains reaching over 2.5 km altitude, and consequently some areas within the Larsen-C Ice Shelf study region have more than 50 m of elevation change within a 1 km^2 area. The Antarctic Peninsula experiences the highest incidence of elevation measurement retrieval failure; however, some of this may be attributable to the 0.2–5 km spatial resolution of the DEM against which the Level 2 CryoSat-2 surface elevation is evaluated (Liu et al., 1999), rather than error in the CryoSat-2 surface elevation measurement. While it is

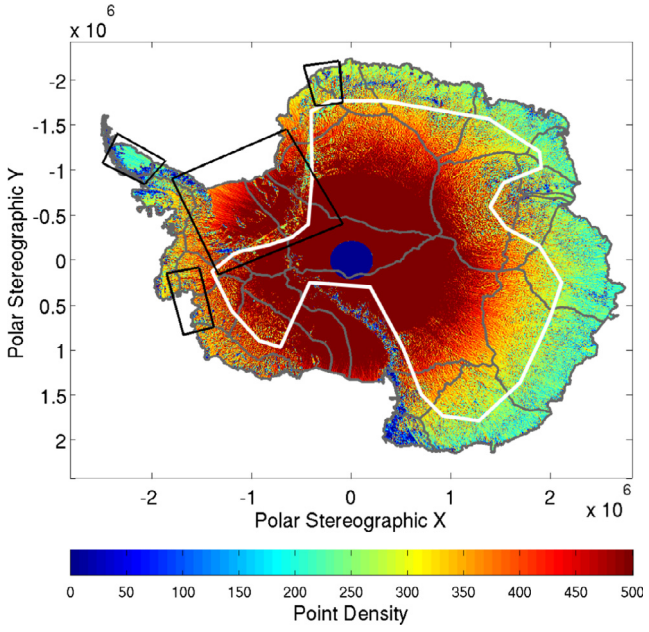

Fig. 2. CryoSat-2 POCA density per 5 km by 5 km grid cell before the plane fit solution is applied. The location of the four study areas (black boxes), drainage basin boundaries (grey) (Zwally et al., 2012) and CryoSat-2 SARIn/LRM mode mask boundary (white) is also shown.

out of the scope of this study to investigate retracker performance, in the future it may be possible to increase the data density of POCA in mountainous regions by evaluating the Level 2 CryoSat-2 surface elevation data quality flag against a finer spatial resolution or more recently acquired DEM as this will reduce the number of L2 elevation data points rejected.

3. Study areas

The CryoSat-2 break in surface slope was produced in four study areas based on their scientific pertinence, availability of evaluation datasets or heterogeneous topography relative to the rest of the Antarctic ice sheet (Fig. 2). The Amundsen Sea sector is grounded on bedrock that lies below current sea level with a topographic gradient that deepens inland towards the Byrd Trench. The region is of particular scientific interest because the low bed elevation allows incursions of warm deep water into the Byrd Trench, making the region unstable and particularly susceptible to uncontrolled grounding line retreat (Favier et al., 2014). Over 30 km of hinge line retreat have been observed in the Amundsen Sea sector over the last two decades (Rignot, 1998b; Park et al., 2013; Rignot et al., 2014), and these observations provide the most extensive grounding line dataset in Antarctica for evaluating the performance of the break in surface slope as a proxy for grounding line position. Conversely the Ekström Ice Shelf study area was selected because of its relative stability, as no significant ice thinning (McMillan et al., 2014) or grounding line retreat has been observed. The Larsen-C Ice Shelf, located on the Antarctic Peninsula, was selected as a study area because the steep mountainous terrain makes it a challenging region for obtaining reliable altimetry surface elevation measurements (Shepherd et al., 2012). Furthermore, in 1995 (Rott et al., 1996) and 2002 (Rack and Rott, 2004) catastrophic ice shelf collapse was observed on the neighbouring Larsen-A and -B Ice Shelves respectively, demonstrating that regular, contemporary observations are required to monitor change in one of the most rapidly evolving sectors of the Antarctic ice sheet. The Filchner-Ronne Ice Shelf was selected as a big ice shelf study area because there is a larger volume of evaluation data available than for the Ross Ice Shelf, as a smaller proportion of the grounding line is located in the Polar data gap which exists north of 81.5° latitude in many sun-synchronous, polar orbiting satellite mission datasets such as ERS-1 and -2.

4. Methods

4.1. Computing ice sheet surface slope

In the Amundsen Sea sector, Larsen-C and Ekström Ice Shelf study areas the corrected and filtered CryoSat-2 data was accumulated into 5 km by 5 km geographical regions on an overlapping grid, with grid centres 1 km by 1 km apart. The grid cell spacing determines the spatial sampling of the CryoSat-2 slope break product, and the cell size governs the data density per grid cell which affects the success of the plane fit solution. We find that a 5 km by 5 km grid provides the best trade-off between coverage and resolution given the volume and spatial coverage of CryoSat-2 SARIn mode data acquired over the ~3.8 year study period. We also use 5 km by 5 km square grid cells in the Filchner-Ronne study area; however, in order to further increase the processing speed for significantly larger areas, we overlap grid cell centres within 10 km of the existing auxiliary QDInSAR hinge line data product (Rignot et al., 2011).

We employed a plane fit solution (Eq. (1)) to compute surface slope in each grid cell in all four study areas (McMillan et al., 2014). Ice surface elevation (z) for each grid cell is computed using the geophysically corrected local mean surface elevation for each POCA ($\bar{z}$), and modelling this as a quadratic function of surface terrain (x, y), a linear function of time (t), and a time-invariant function of satellite heading (h) based on the anisotropy in the ascending and descending satellite passes (McMillan et al., 2014). A backscatter (s) term is also included to account for time varying properties of the ice sheet surface.

$$z = \bar{z} + a_0x + a_1y + a_2t + a_3h + a_4s \quad (1)$$

Data points deemed to be outliers were culled if there was more than 5 m difference from the modelled surface, and the plane fit solution was iterated for each 5 × 5 km grid cell until no more data points were removed. After iteration, the model solution was retained for each individual grid cell if the CryoSat-2 data density is greater than 8 points, and if a time period of 2 years or more is spanned to minimise the influence of short term change. Surface slope was calculated as the gradient of the model plane within each grid cell (Fig. 3a), and inverse-distance 2D weighted interpolation was used to fill in any remaining gaps in the slope map. In the largest area of interest considered in this study, the Filchner-Ronne Ice Shelf, interpolation was required in 8.5% of the grid cells. Error in the plane fit solution primarily depends on the spatial distribution of elevation measurements accumulated within each grid cell (McMillan et al., 2014). The error will be significantly larger in areas of heterogeneous terrain where a simple 2D planar surface does not fully represent the spatial variability of the ice surface. Surface elevation and slope data retrieved from a transect across the Filchner-Ronne Ice Shelf illustrates that the QDInSAR hinge line corresponds with the point of most rapid change in surface elevation (Fig. 3b) and surface slope (Fig. 3c). At all four locations where the QDInSAR hinge line intersects the 1090 km long transect, the most rapid change in surface slope (Fig. 3c) corresponds with a peak in the derivative of the absolute surface slope, termed the slope break (Fig. 3d), greater than 0.1°. Slope break (Figs. 3d and 4c) is a more variable measurement than surface slope (Figs. 3c and 4b) because mountainous terrain far inland of the grounding line exhibits large change in surface slope relative to flat ice shelves.

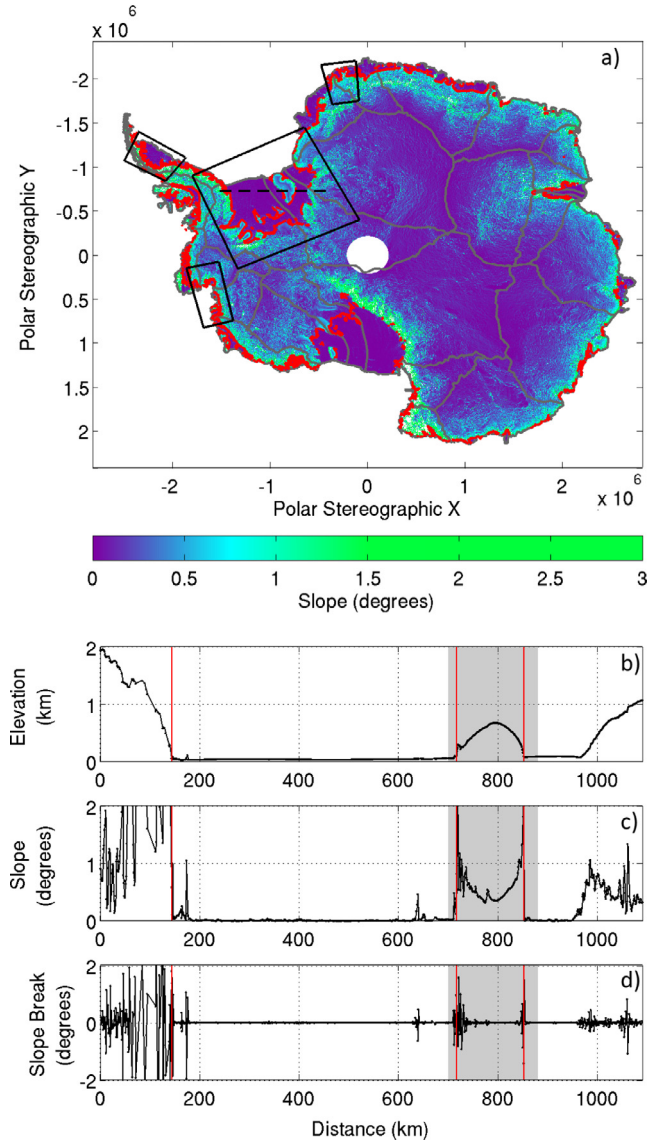

Fig. 3. (a) Antarctic ice sheet and ice shelf surface slope measured by CryoSat-2. Also shown are drainage basins (grey) (Zwally et al., 2012), hinge line determined from QDInSAR (red) (Rignot et al., 2011) and the four regions considered in detail in this study (black box). Ice surface elevation (b), slope (c) and slope break (d) along a profile of the Filchner-Ronne Ice Shelf (black dashed line in a), shown relative to the QDInSAR hinge line crossing points (vertical red lines). The grey shaded area (b, c, d) is highlighted in Fig. 4, and indicates the location of Berkner Island on the transect.

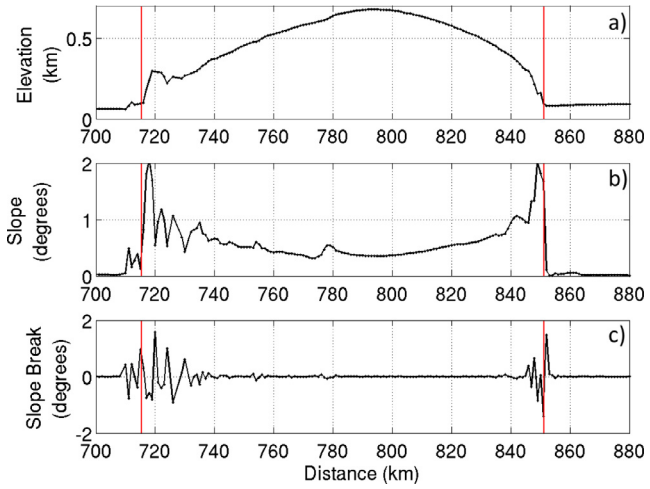

Fig. 4. Ice surface elevation (a), slope (b) and slope break (c) across Berkner Island on the Filchner-Ronne Ice Shelf (grey shaded area in Fig. 3b), shown relative to the QDInSAR hinge line crossing points (vertical red lines).

As the slope break and point of most rapid change in surface slope correspond, we pick the position, termed the CryoSat-2 break in surface slope, where surface slope exceeds a specified value, enabling a range of slope values to be evaluated and optimised relative to the QDInSAR hinge line position.

4.2. Identification of break in surface slope

As a first step towards locating the break in surface slope, we investigated the range of slopes determined from the CryoSat-2 data in the vicinity of the grounded ice boundary to assess their spatial variability and therefore sensitivity. In areas with very steep surface slopes there is a very small change in position of the break in surface slope picked at different slope values; however, in regions with shallow surface slope there is a much larger separation. For intercomparison, we used hinge line locations mapped between 1992 and 2009 using QDInSAR (Rignot et al., 2011). Although there has been rapid grounding line retreat in parts of the Amundsen Sea sector, the majority of our study area has been in a state of approximate balance according to satellite observations of ice thickness change (Shepherd et al., 2012; McMillan et al., 2014), and so the 17 year mismatch between the two datasets should not adversely affect this assessment as it can be assumed that the surface terrain has not changed. The vast majority of all hinge line positions are located on ice exhibiting very low surface slopes, with over 70% falling on slopes of less than 1.0° in all 4 study areas (Fig. 5), where Ekström Ice Shelf had the lowest percentage (70.3%) and Filchner-Ronne Ice Shelf the highest (76.0%).

Taking the range of hinge line slopes into account, we generated contours at 0.1° intervals using a bilinear interpolation scheme to define a continuous line passing between common values of the surface slope. Some line breaks did occur, and so it was necessary to connect open contours separated by small gaps (<25 km) at their closest point. Connecting contour breaks was mainly required on high slope terrain (>0.5°), and illustrates that for this method the continuity of the grounded ice boundary is dependent upon the steepness of the local terrain. It was not possible to produce a continuous contour for slopes greater than 0.9° on the Ekström Ice Shelf, 0.8° in the Amundsen Sea sector, and 0.7° on the Filchner-Ronne Ice Shelf, as the surface slopes were not persistently high

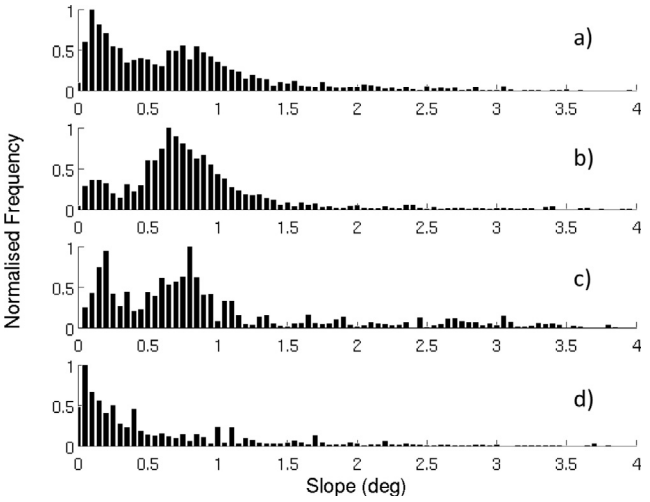

Fig. 5. Distribution of the ice surface slope retrieved at the QDInSAR grounding line in the Amundsen Sea sector (a), Larsen-C Ice Shelf (b), Ekström Ice Shelf (c) and the Filchner-Ronne Ice Shelf (d) (Fig. 2).

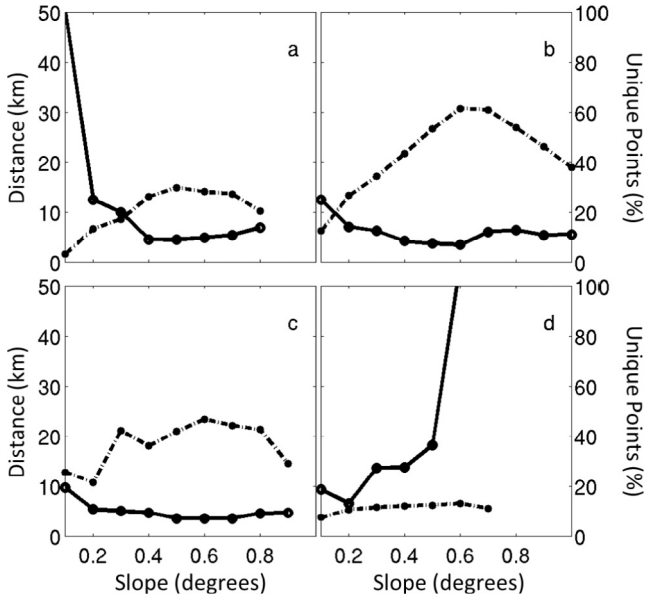

Fig. 6. Mean absolute separation between the ice sheet hinge line, as determined from QDInSAR (Rignot et al., 2011) and contours of the ice sheet surface slope, as determined from CryoSat-2 altimetry in (a) the Amundsen Sea sector, (b) Larsen-C Ice Shelf, (c) Ekström Ice Shelf, and (d) Filchner-Ronne Ice Shelf (solid black line). Also shown is the number of unique points used in each comparison (dashed black line).

enough around large proportions of the coast. We excluded contours surrounding areas smaller than 1000 km^2 as being not representative of the main ice sheet. Although this data editing step is designed to remove boundaries associated with erroneous data, it does also limit the utility of the approach for identifying relatively small regions of grounded ice within floating ice shelves such as ice rises.

To assess the similarity between the hinge line and break in surface slope, we calculated the mean absolute separation between each point on the QDInSAR hinge line and the nearest point on each slope contour in all four study areas (Fig. 6). We used the QDInSAR hinge line dataset to perform this assessment because it is the most direct and cotemporaneous measurement of the grounding line, in comparison with the position obtained from other techniques. In the Amundsen Sea sector the mean separation of the QDInSAR hinge line to the CryoSat-2 break in surface slope is over 50 km for the 0.1° slope value; however, for slope values between 0.3° and 0.8° the mean separation is less than 10 km. The Ekström Ice Shelf exhibits a similar pattern to the Amundsen Sea sector study area with a larger separation measured at lower slope values. However, there is less than 0.01 km difference in the mean separation of the break in surface slope determined from values between 0.5° and 0.7°, indicating that in the Ekström Ice Shelf study area the break in surface slope is less sensitive to the optimum slope value. The Larsen-C Ice Shelf region is characterised by steep mountainous terrain typical of the Antarctic Peninsula. Evaluation of the break in surface slope in this region shows that there is over 5 km separation between the QDInSAR hinge line for slope values less than 0.4° or greater than 0.6°. However, the separation of the hinge line and the break in surface slope determined from 0.5° and 0.6° slope values exhibit root mean square variability of less than 5 km, suggesting that the performance of the technique is particularly good in this region.

Contrary to the three other study areas, for the Filchner-Ronne Ice Shelf the mean separation of the QDInSAR hinge line and the CryoSat-2 break in surface slope increases with increasing slope values. Slope values equal to and less than 0.2° result in a mean separation of less than 10 km indicating that much lower surface slopes are characteristic of this large study area resulting in a significantly lower optimum slope value. The number of unique points (Fig. 6) provides, additionally, an indication of the completeness of each contour and of the confidence of the inter-comparison. In general, the largest number of unique matches between data points on the slope contours, and the hinge line validation data set, occur with slopes in the range of 0.2–0.8°. For values outside this range, the inter-comparison can be considered less robust. The CryoSat-2 break in surface slope that matches most closely with the hinge line position is determined from slope values of 0.5°, 0.6°, 0.5° and 0.2° in the Amundsen Sea sector, Larsen-C, Ekström and Filchner-Ronne ice shelves respectively (Fig. 6).

Although there are regional differences in the slope value that marks the break in surface slope optimised against the QDInSAR hinge line, only the Filchner-Ronne Ice Shelf shows a significant departure from the mean. In the Filchner-Ronne Ice Shelf study area the smallest mean absolute separation from the QDInSAR hinge line occurs at the CryoSat-2 break in surface slope produced from low slope values, less than 0.3°. However, a different slope regime is exhibited in the three other study areas where a larger mean absolute separation is measured for slopes less than 0.3°. This is in part explained by the presence of stee-

ply sloping mountainous terrain in the Larsen-C and Ekström Ice Shelf study areas, and high rates of basal shear in the Amundsen Sea sector which result in evolution and steepening of the ice surface geometry (Payne et al., 2004; Joughin et al., 2010). The influence of topographic and basal shear controls on surface geometry is less significant in large central and western sectors of the Filchner-Ronne Ice Shelf study area, as shown by spatially extensive lower slope measurements inland of the grounding line (Fig. 3a). This provides additional evidence that a different slope regime is found in the Filchner-Ronne Ice Shelf study area. Furthermore, the Amundsen Sea sector, Larsen-C Ice Shelf and Ekström Ice Shelf study areas show a very small difference between the minimum separation measured at the 0.4°, 0.5° and 0.6° slope boundary with a mean separation of less than 5 km measured for all three slope values, and a total range in the separation of all data points of 1.5 km. Given that the area of these three regions is significantly smaller than the Filchner-Ronne Ice Shelf study area, and that individually the slope regimes are similar with low root mean square variability at the optimum slope value, we combined the three study areas in order to pick the break in surface slope at a more widely applicable optimum value. The optimum slope value determined by a linear fit to each dataset is 0.2° for the Filchner-Ronne Ice Shelf, and 0.5° for all three other study areas (Fig. 7).

5. Results and discussion

We mapped the location of the break in surface slope, determined by contouring slope values of 0.2° at the Filchner Ronne Ice Shelf and as the 0.5° elsewhere (Fig. 8).

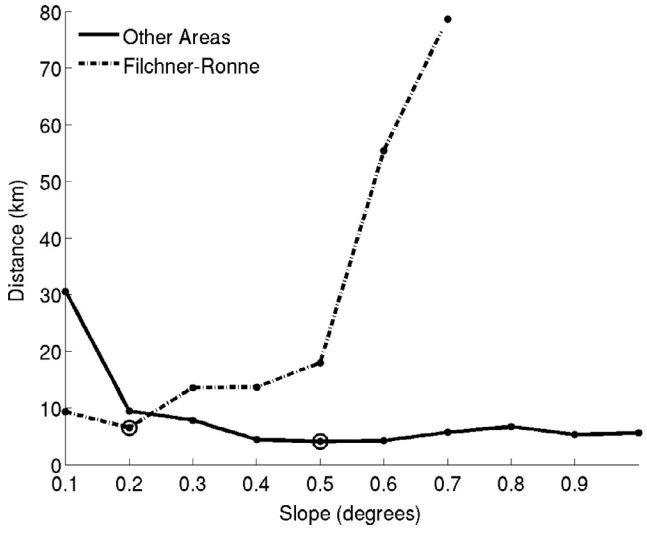

Fig. 7. Optimum slope values (large black circle) determined as the minimum mean absolute separation between the QDInSAR hinge line (Rignot et al., 2011) and the break in surface slope determined from CryoSat-2 SARIn altimetry. The Amundsen Sea sector, Ekström Ice Shelf and Larsen-C Ice Shelf are grouped together (solid black line) whereas the Filchner-Ronne Ice Shelf which has a different slope regime is shown separately (dashed black line).

Apart from a 55 km section of the Filchner-Ronne Ice Shelf, across the Foundation ice stream (−82.6 S, −60.3 W) where no CryoSat-2 SARIn data were acquired prior to 2013, the remaining 8600 km of this boundary is continuous. We compared the CryoSat-2 break in surface slope to independent grounding line proxy datasets, including the QDInSAR hinge line (Rignot et al., 2011) and the shadow edge boundary (Bindschadler et al., 2011). The spatial separation between the CryoSat-2 break in surface slope and the QDInSAR hinge line (Fig. 8) shows that on average for all four study areas, the mean absolute separation is 4.5 km, with differences of 6.5 km, 3.5 km, 4.5 km and 3.7 km in the Filchner-Ronne Ice Shelf, Ekström Ice Shelf, Amundsen Sea sector and Larsen-C Ice Shelf respectively (Table 2). The regional mean separation between the CryoSat-2 break in surface slope and shadow edge boundary is smaller, at 3.1 km, 2.6 km 3.8 km and 3.0 km for the Filchner-Ronne Ice Shelf, Ekström Ice Shelf, Amundsen Sea sector and Larsen-C Ice Shelf respectively. The close correspondence between the topographic break in surface slope and the shadow edge boundary provides supporting evidence that both datasets can be used as a proxy for each other. The overall mean difference between the CryoSat-2 break in surface slope and shadow edge boundary is 3.1 km, 1.4 km less than the difference between the QDInSAR hinge line and shadow edge boundary validation datasets (Table 2) which differ by 4.5 km on average for all four study areas.

A zoomed in view of the CryoSat-2 grounded ice boundary on the Filchner-Ronne Ice Shelf shows agreement between the break in surface slope and QDInSAR techniques across ice streams such as Carlson Inlet; around isolated ice rises in the centre of the ice shelf such as Henry Ice Rise; and across ice streams where no QDInSAR estimate exists such as Baily and Slessor Ice Streams (Fig. 9).

We evaluated the location of the CryoSat-2 break in surface slope against estimates of the grounding line position produced from independent satellite datasets and techniques. The QDInSAR hinge line is produced from ERS-1/2 and ALOS PALSAR SAR data acquired between 1992 and 2009 (Rignot et al., 2011), and the shadow edge boundary is produced from a combination of optical Landsat 7+ and laser altimetry ICESat data acquired between 1999 and 2009 (Fricker and Padman, 2006; Bindschadler et al., 2011). The CryoSat-2 data used in this study was acquired between 2010 and 2014, therefore neither of the available evaluation datasets are contemporaneous. This is an important consideration in areas of rapid grounding line retreat such as the Amundsen Sea sector (Park et al., 2013) where grounding line retreat of up to 35 km, and maximum rates of 1.8 km per year, have been observed over the last 25 years (Rignot et al., 2014). It is important to note that, while in the Amundsen Sea sector some of the difference between the CryoSat-2 break in surface slope and the QDInSAR hinge line products can be attributed to change over time, this is unlikely to be true in other more stable regions such as the Ekström Ice Shelf where dynamic

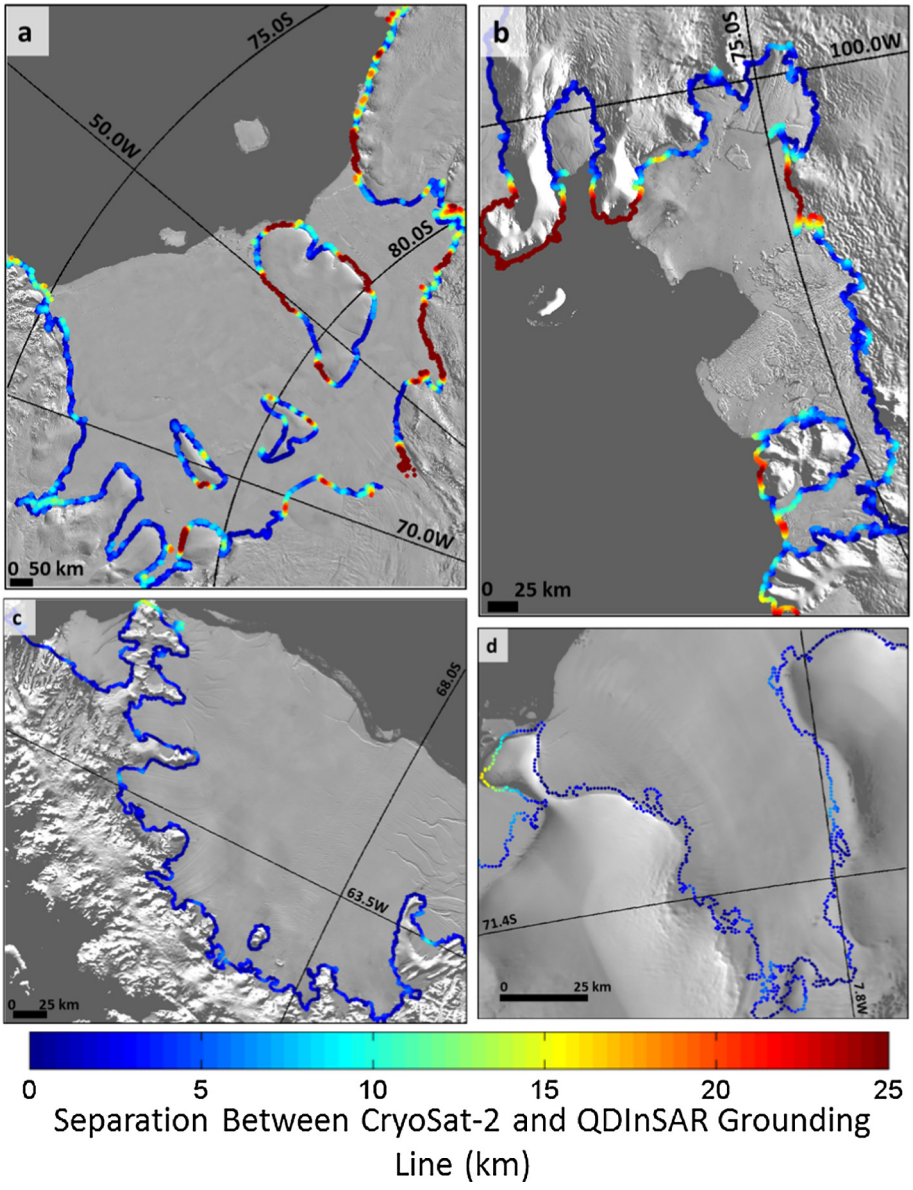

Fig. 8. CryoSat-2 break in surface slope in the Filchner-Ronne Ice Shelf (a), Amundsen Sea sector (b), Larsen-C Ice Shelf (c) and Ekström Ice Shelf (d) study areas, colour scaled to show mean absolute separation from the QDInSAR hinge line.

imbalance has not occurred. In these regions the separation between the CryoSat-2 break in surface slope and the evaluation datasets is more likely attributable to measurement inaccuracy. In all study areas and for all techniques the standard deviation of the separation is greater than the mean (Table 2). The greatest variability (68.8 km) which occurs between the QDInSAR and shadow edge boundary products on the Filchner-Ronne Ice Shelf (Table 2), is caused by a previously documented misplacement of the grounding line position on Slessor Glacier (Rignot et al., 2011). Overall, in all four study areas 82% of the CryoSat-2 break in surface slope is separated by less than 10 km from the QDInSAR hinge line demonstrating the agreement between both techniques (Fig. 10).

We evaluated the difference between the CryoSat-2 break in surface slope and the QDInSAR hinge line position in the Amundsen Sea sector in more detail as this is the only region where rapid grounding line retreat has been observed and a time series of QDInSAR hinge line measurements exist. The results show that, across the main trunk of the Pine Island Glacier in the Amundsen Sea sector, West Antarctica, the break in surface slope is further inland than the QDInSAR hinge line produced in 2000, but corresponds well with the 2011 QDInSAR hinge line (Fig. 11a) (Rignot et al., 2014). Thwaites Glacier is another region of known grounding line retreat and here the CryoSat-2 break in surface slope also more closely matches the spatial location and complex pattern of the 2011

Table 2
Separation between estimates of grounding line position produced from the QDInSAR hinge line (Rignot et al., 2011), the shadow edge boundary (Bindschadler et al., 2011), and the CryoSat-2 break in surface slope, in all four study areas.

Region	CryoSat-2 break in surface slope to QDInSAR hinge line		CryoSat-2 break in surface slope to shadow edge boundary		QDInSAR hinge line to shadow edge boundary	
	Mean separation (km)	Standard deviation of separation (km)	Mean separation (km)	Standard deviation of separation (km)	Mean separation (km)	Standard deviation of separation (km)
Filchner-Ronne	6.5	10.6	3.1	3.9	3.9	68.8
Ekström	3.5	7.2	2.6	2.0	5.8	10.2
Amundsen	4.5	7.1	3.8	3.9	6.2	12.5
Larsen-C	3.7	3.8	3.0	4.6	2.4	7.2

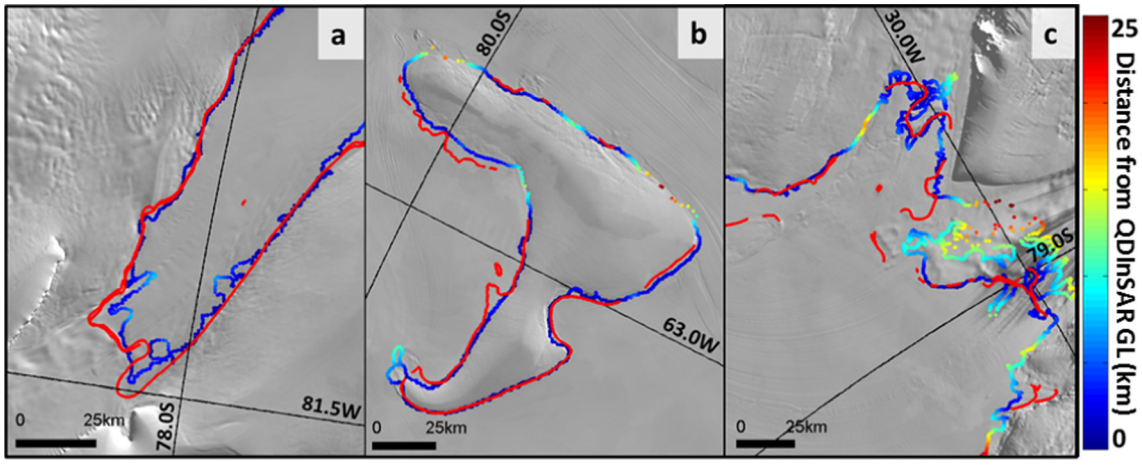

Fig. 9. Grounded ice boundary from the CryoSat-2 break in surface slope colour scaled to show mean absolute separation from the QDInSAR hinge line in three diverse areas of the Filchner-Ronne Ice Shelf including Carlson Inlet (a), Henry Ice Rise (b), Baily and Slessor Ice Streams (c). The location of the QDInSAR grounding line is also shown (red) (Rignot et al., 2011).

QDInSAR hinge line (Rignot et al., 2014) compared to the 1996 QDInSAR hinge line position (Rignot et al., 2011) (Fig. 11b). Smith Glacier is the most rapidly thinning ice stream in Antarctica, with surface lowering rates of up to 9 m per year measured since 2010 (McMillan et al., 2014). In comparison to the 1995 QDInSAR hinge line position, ~19.1 km of inland retreat of the ice shelf boundary is measured by the CryoSat-2 break in surface slope; however, this is ~12.3 km less than the 2011 QDInSAR hinge line position compared with the same 1995 dataset (Rignot et al., 2014) (Fig. 11c). Despite the difference in inland retreat, the CryoSat-2 break in surface slope result shows that the zone of retreat extends an additional 25.6 km across Pope Glacier in the Amundsen Sea sector, West Antarctica, a region that was unable to be mapped in 2011 due to lack of coherent SAR data. The CryoSat-2 break in surface slope shows that ~9.6 km of grounding line migration has occurred on Pope Glacier since the 1995, extending the zone of grounding line retreat to better match the observed region of surface lowering (McMillan et al., 2014).

Our CryoSat-2 break in surface slope product provides a contemporary update to previous estimates of the grounding line position based on the QDInSAR hinge line and shadow edge boundary techniques. These results provide a more recent assessment of the Antarctic ice sheet grounding line position compared with the most recent QDInSAR hinge line positions, measured in 2011 in the Amundsen Sea sector (Park et al., 2013; Rignot et al., 2014), 2009 on the Filchner-Ronne Ice Shelf, 2000 on the Ekström Ice Shelf and 1996 on the Larsen-C Ice Shelf (Rignot et al., 2011). The CryoSat-2 break in surface slope confirms that, in regions of sustained grounding line retreat, the present day break in surface slope is further inland than historical QDInSAR hinge line measurements. Furthermore CryoSat-2 extends the region of contemporary retreat to encompass Pope Glacier which has thinned rapidly in the last 5 years (McMillan et al., 2014), an ice stream where the QDInSAR hinge line has not been mapped within the last 20 years. The spatial resolution (30 m) and vertical accuracy (3.7 cm) of the QDInSAR technique is unprecedented (Hogg et al., 2016), and when coherent SAR images

are acquired they will serve as the primary hinge line measurement. However, over the last 25 years suitable data has not been acquired over the full Antarctic ice sheet and, outside of the Amundsen Sea sector, observations of grounding line retreat are universally sparse.

We mapped the break in surface slope using a new independent technique which utilises CryoSat-2 radar altimetry data in four large, key study areas around the Antarctic ice sheet. The break in surface slope has previously been mapped using the shadow edge boundary as a proxy (Scambos et al., 2007; Bindschadler et al., 2011); however, we provide the first assessment of using a direct measurement of the break in surface slope derived from geodetic surface elevation data as a proxy for a continuous ice sheet grounding line. Historical radar altimeter missions such as ERS-1/2 and ENVISAT, and in the future Sentinel-3, combine to provide the most spatially wide, and temporally dense and continuous time series of ice sheet observations acquired by any instrument to date. In the future it will be possible to exploit the radar altimetry data archive to produce a 25 year long time series of the grounded ice boundary from the break in surface slope, although the earlier satellite missions will not benefit from the improved spatial sampling, smaller footprint size and improved elevation accuracy afforded by the CryoSat-2 SARIn mode. This will provide an independent, complimentary means of detecting long term change in the grounded ice boundary location, both in regions of known instability such as West Antarctica, and in areas such as East Antarctica where SAR data required for the QDInSAR technique has not been acquired. CryoSat-2's novel SARIn mode, together with its unique orbit combine to enable acquisition of spatially dense elevation measurements from which a relatively high resolution surface elevation map can be produced. The wider ~3 km track spacing of traditional pulse limited altimeters will limit the spatial resolution of a historical product for break in surface slope; however, DEMs of geodetic surface heights could also be used to improve the spatial resolution. In the future it may be possible to directly compare cotemporaneous QDInSAR hinge lines with the break in surface slope, if the CryoSat-2 mission lifetime overlaps sufficiently with Sentinel-1b. This will enable short (6-day) repeat period SAR triplets to be acquired, which may be suitable for quadruple difference interferometry.

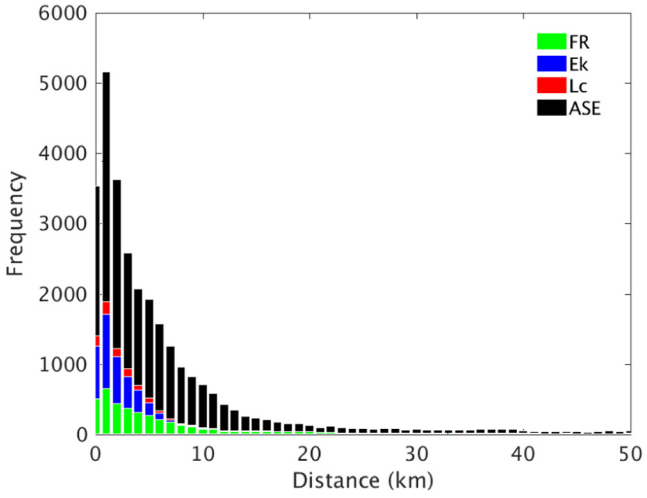

Fig. 10. Separation of the CryoSat-2 break in surface slope from the QDInSAR hinge line in all four study areas, where 82% of the total dataset is separated by less than 10 km.

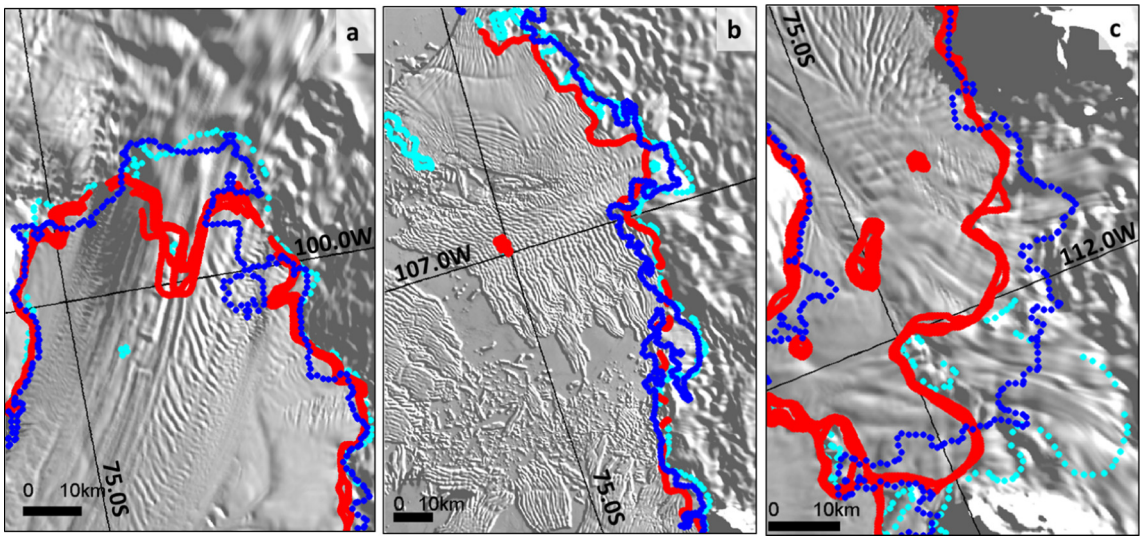

Fig. 11. CryoSat-2 break in surface slope (blue) on Pine Island Glacier (a), Thwaites Glacier (b) and Smith and Pope Glaciers (c) in the Amundsen Sea sector, West Antarctica, shown alongside QDInSAR hinge line produced from SAR data acquired between 1992 and 2009 (red) and the 2011 (cyan) (Rignot et al., 2014).

6. Conclusions

We have measured the break in surface slope from CryoSat-2 radar altimetry data using an automated and computationally efficient plane fit solution. The dense spatial sampling of the CryoSat-2 SARIn mode in the ice sheet margins (McMillan et al., 2014) has enabled a measurement of the break in surface slope to be produced every 1 km. Good agreement was found between the CryoSat-2 break in surface slope and the validation QDInSAR hinge line in all four study areas, with average separation of 6.5 km, 3.5 km, 4.5 km and 3.7 km on the Filchner-Ronne Ice Shelf, Ekström Ice Shelf, Amundsen Sea sector and the Larsen-C Ice Shelf respectively. The separation between the CryoSat-2 break in surface slope and optical grounded ice boundary is even smaller at 3.1 km on average, and the mean absolute separation between the two independent evaluation datasets (4.5 km) indicates that the CryoSat-2 break in surface slope is of comparable accuracy to the existing datasets. In regions of rapid change such as the Amundsen Sea sector, the CryoSat-2 break in surface slope more closely matches the published 2011 QDInSAR hinge line position in comparison to the historical position measured from data acquired 10 years earlier. This provides confidence that the CryoSat-2 break in surface slope correlates well with the present day QDInSAR hinge line location and can act as a complimentary new proxy measurement of the ice sheet grounding line. In future this method could be extended to map the break in surface slope for the entire perimeter of the Antarctic ice sheet using CryoSat-2. This new technique is automated, quick to run and objective. Therefore, when more data is acquired by CryoSat-2 in the future, it may also be possible to monitor change in the break in surface slope position using radar altimetry data.

Acknowledgements

This work was performed by AH, AS, LG, AM and MD during the ESA CryoSat+ Cryosphere GLITter Study (Contract C 4000107395), and the ESA CryoSat+ Cryo-Top Evolution Study, with support from ESA's Support To Science Element (STSE) and a NERC studentship. We thank ESA for acquiring and supplying the CryoSat-2 satellite dataset which formed the basis of this study.

References

Bindschadler, R., Choi, H., Wichlacz, A., Bingham, R., Bohlander, J., Brunt, K., Corr, H., Drews, R., Fricker, H., Hall, M., Hindmarsh, R., Kohler, J., Padman, L., Rack, W., Rotschky, G., Urbini, S., Vornberger, P., Young, N., 2011. Getting around Antarctica: new high-resolution mappings of the grounded and freely-floating boundaries of the Antarctic ice sheet created for the International Polar Year. The Cryosphere 5, 569–588.

Bohlander, J., Scambos, T., 2007. Antarctic Coastlines and Grounding Line Derived from MODIS Mosaic of Antarctica (MOA), Boulder, Colorado USA: National Snow and Ice Data Center, Digital Media (accessed 1st September 2016).

Brunt, K.M., Fricker, H.A., Padman, L., Scambos, T.A., O'Neel, S., 2010. Mapping the grounding zone of the Ross Ice Shelf, Antarctica using ICESat laser altimetry. Ann. Glaciol. 51 (55), 71–79.

Brunt, K.M., Fricker, HA., Padman, L., 2011. Analysis of ice plains of the Filchner-Ronne Ice Shelf, Antarctica, using ICESat laser altimetry. J. Glaciol. 57 (205), 965–975.

CryoSat-2 Product Handbook, 2012. ESRIN-ESA and Mullard Space Science Laboratory – University College London. <http://emits.sso.esa.int/emits-doc/ESRIN/7158/CryoSat-PHB-17apr2012.pdf>.

Dutrieux, P., De Rydt, J., Jenkins, A., Holland, P.R., Ha, H.K., Lee, S.H., Steig, E.J., Ding, Q., Abrahamsen, E.P., Shröder, M., 2014. Strong sensitivity of Pine Island Ice-Shelf melting to climatic variability. Science 343, 174–178. http://dx.doi.org/10.1126/science.1244341.

Favier, L., Durand, G., Cornford, S.L., Gudmundsson, G.H., Gagliardini, O., Gillet-Chaulet, F., Zwinger, T., Payne, A.J., Le Brocq, A.M., 2014. Retreat of Pine Island Glacier controlled by marine ice-sheet instability. Nat. Clim. Change 4, 117–121. http://dx.doi.org/10.1038/NCLIMATE2094.

Fricker, H.A., Padman, L., 2006. Ice shelf grounding zone structure from ICESat laser altimetry. Geophys. Res. Lett. 33, L15502.

Fricker, H.A., Coleman, R., Padman, L., Scambos, T.A., Bohlander, J., Brunt, K.M., 2009. Mapping the grounding zone of the Amery Ice Shelf, East Antarctica using InSAR, MODIS and ICESat. Antarct. Sci. 21 (5), 515–532.

Hogg, A.E., Shepherd, A., Gourmelen, N., Engdahl, M., 2016. Grounding line migration from 1992 to 2011 on Petermann Glacier, North-West Greenland. J. Glaciol. 62 (236), 1104–1114. http://dx.doi.org/10.1017/jog.2016.83.

Horgan, H.J., Anandakrishnan, S., 2006. Static grounding lines and dynamic ice streams: evidence from Siple Coast, West Antarctica. Geophys. Res. Lett. 33, L18502. http://dx.doi.org/10.1029/2006GL027091.

Joughin, I., Smith, B.E., Holland, D.M., 2010. Sensitivity of 21st century sea level to ocean induced thinning of Pine Island Glacier, Antarctica. Geophys. Res. Lett. 37, L20502. http://dx.doi.org/10.1029/2010GL044819.

Joughin, I., Alley, R.B., Holland, D.M., 2012. Ice-sheet response to oceanic forcing. Science 338, 1172–1176. http://dx.doi.org/10.1126/science.1226481.

Joughin, I., Smith, B.E., Medley, B., 2014. Marine ice sheet collapse potentially underway for the Thwaites Glacier basin, West Antarctica. Science 344, 735–738. http://dx.doi.org/10.1126/science.1249055.

Liu, H., Jezek, K., Li, B., 1999. Development of an Antarctic digital elevation model by integrating cartographic and remotely sensed data: a geographic information system based approach. J. Geophys. Res. 104 (B10), 199–213. http://dx.doi.org/10.1029/1999JB900224.

McMillan, M., Shepherd, A., Nienow, P., Leeson, A., 2011. Tide model accuracy in the Amundsen Sea, Antarctica, from radar interferometry observations of ice shelf motion. J. Geophys. Res. 116, C11008. http://dx.doi.org/10.1029/2011JC007294.

McMillan, M., Shepherd, A., Sundal, A., Briggs, K., Muir, A., Ridout, A., Hogg, A., Wingham, D., 2014. Increased ice losses from Antarctica detected by CryoSat-2. Geophys. Res. Lett. 41, 3899–3905.

Padman, L., Fricker, H.A., Coleman, R., Howard, S., Erofeeva, S., 2002. A new tidal model for the Antarctic ice shelves and seas. Ann. Glaciol. 34, 247–254.

Park, J.W., Gourmelen, N., Shepherd, A., Kim, S.W., Vaughan, D.G., Wingham, D.J., 2013. Sustained retreat of the Pine Island Glacier. Geophys. Res. Lett. 40, 2137–2142.

Payne, A.J., Vieli, A., Shepherd, A.P., Wingham, D.J., Rignot, E., 2004. Recent dramatic thinning of largest West Antarctic ice stream triggered by oceans. Geophys. Res. Lett. 31, L23401. http://dx.doi.org/10.1029/2004GL021284.

Rack, W., Rott, H., 2004. Pattern of retreat and disintegration of the Larsen-B ice shelf, Antarctic Peninsula. Ann. Glaciol. 39, 505–510.

Rignot, E., 1998a. Hinge-line migration of Petermann Gletscher, North Greenland, detected using satellite-radar interferometry. J. Glaciol. 44 (148), 469–476.

Rignot, E., 1998b. Fast recession of a West Antarctic Glacier. Science 281, 549–551.

Rignot, E., Mouginot, J., Scheuchl, B., 2011. Antarctic grounding line mapping from differential satellite radar interferometry. Geophys. Res. Lett. 38, L10504.

Rignot, E., Mouginot, J., Morlighem, M., Seroussi, H., Scheuchl, B., 2014. Widespread, rapid grounding line retreat of Pine Island, Thwaites, Smith, and Kohler glaciers, West Antarctica, from 1992 to 2011. Geophys. Res. Lett. 41, 3502–3509. http://dx.doi.org/10.1002/2014GL060140.

Rott, H., Skvarca, P., Nagler, T., 1996. Rapid collapse of Northern Larsen Ice Shelf, Antarctica. Science 271 (5250), 788–792.

Scambos, T.A., Haran, T.M., Fahnestock, M.A., Painter, T.H., Bohlander, J., 2007. MODIS-based Mosaic of Antarctica (MOA) data sets: continent-wide surface morphology and snow grain size. Rem. Sens. Environ. 111 (2–3), 242–257.

Schoof, C., 2007. Ice sheet grounding line dynamics: steady states, stability and hysteresis. J. Geophys. Res. 112, F03S28.

Shepherd, A., Ivins, E.R., Barletta, G.A.V.R., Bentley, M.J., Bettadpur, S., Briggs, K.H., Bromwich, D.H., Forsberg, R., Galin, N., Horwath, M., Jacobs, S., Joughin, I., King, M.A., Lenaerts, J.T.M., Li, J., Ligtenberg, S.R.M., Luckman, A., Luthcke, S.B., McMillan, M., Meister, R., Milne, G., Mouginot, J., Muir, A., Nicolas, J.P., Paden, J., Payne, A.J., Pritchard, H., Rignot, E., Rott, H., Sørensen, L.S., Scambos, T.A., Scheuchl, B., Schrama, E.J.O., Smith, B., Sundal, A. V., van Angelen, J.H., van de Berg, W.J., van den Broeke, M.R., Vaughan, D.G., Velicogna, I., Wahr, J., Whitehouse, P.L., Wingham, D.J., Yi, D., Young, D., Zwally, H.J., 2012. A reconciled estimate of ice-sheet mass balance. Science 338, 1183–1189. http://dx.doi.org/10.1126/science.1228102.

Thomas, R.H., Sanderson, T.J.O., Rose, K.E., 1979. Effect of climatic warming on the West Antarctic ice sheet. Nature 277, 355–358.

Vaughan, D.G., 1995. Tidal flexure at ice shelf margins. J. Geophys. Res. 100 (B4), 6213–6224.

Wingham, D.J., Francis, C.R., Baker, S., Bouzinac, C., Brockley, D., Cullen, R., de Chataeu-Thierry, P., Laxon, S.W., Mallow, U., Mavrocordatos, C., Phalippou, L., Ratier, G., Rey, L., Rostan, F., Viau, P., Wallis, D.W., 2006. CryoSat: a mission to determine the fluctuations in Earth's land and marine ice fields. Adv. Space Res. 37, 841–871.

Zwally, H.J., Giovinetto, M.B., Beckley, M.A., Saba, J.L., 2012. Antarctic and Greenland Drainage Systems, GSFC Cryospheric Sciences Laboratory. <http://icesat4.gsfc.nasa.gov/cryo_data/ant_grn_drainage_systems.php>.